

Robust Control of an Electrostatic Microelectromechanical Actuator

M. Karkoub^{*1} and M. Zribi²

¹Mechanical Engineering Department, The Petroleum Institute, Abu Dhabi, UAE

²Electrical Engineering Department, Kuwait University, Kuwait

Abstract: A continuing trend these days is the use of micro-electro-mechanical actuators with electronic circuitry to fabricate MEMS devices such as micro-switches, hard disks, optical micro-mirrors ... One of the problems with the electrostatic MEMS actuator is that when an electrical voltage is applied to these devices, the micro-actuators undergo a residual vibration before reaching their permanent position. This paper addresses the control of an electrostatic microelectromechanical actuator to reduce the vibration effect on its performance. A feedback linearization controller, a static sliding mode controller and a dynamic sliding mode controller are designed for the microelectromechanical system. The stability of the closed loop system is proved. Simulation results indicate that the proposed control schemes work well.

Keywords: Robust control, electrostatic, microelectromechanical actuator.

INTRODUCTION

Micro-Electro-Mechanical Systems (MEMS) have been the subject of a lot of research in the past 50 years or so and a variety of devices have been developed in many fields such as biomedical, automotive, and robotics. Among these devices one finds pressure sensors, discrete acceleration sensors, integrated acceleration sensors, and integrated rate/gyro sensors. One actuator that has proven to be useful in MEMS applications is the Electrostatic type. There are two types of electrostatic actuators: gap-controlled and area-controlled. The gap-controlled actuator is commanded by varying the distance between its electrodes whereas the area-controlled type is governed by changing the overlapping region between the electrodes. The secret behind electrostatic actuators are the coulomb forces that develop between capacitively-coupled conductors differing in voltage. What makes these types of actuators popular is the fact they have simple structure and may be fabricated from standard, well-understood, materials.

The dynamics of the electrostatic actuators is highly nonlinear due the nature of the electrostatic force on the top plate and presents a challenge to researchers. Open-loop control of this type of actuators has proven to be extremely difficult especially over a large operating range. Therefore, researchers have tried to command these actuators through closed-loop control and that technique also has its share of problems. When controlled through the electrode voltage, the nonlinearity gives rise to a saddle-node bifurcation called pull-in which severely limits the operation of the electrostatic actuators. Another major problem that MEMS researchers have faced with electrostatic actuators is that during analog set-point operation with constant voltage bias, the nominal capacitive gap must be at least three times larger than the required range of motion to prevent pull-in. Increas-

ing the capacitive gap complicates the fabrication process and requires higher operating power. Eliminating the pull-in or snap-through effect can increase the range of the movable electrode considerably. Moreover, in the absence of pull-in, disturbances will not cause the movable electrode to depart from its stable operating region and no motion limiters and/or anti-stiction measures are necessary. Many researchers tried to get around the pull-in problem by designing bi-stable digital devices which exploit the bifurcation in the system. The strategy proved to be successful and resulted in numerous research prototypes and commercial devices [1, 2]. Although bi-stable digital devices performed remarkably well, the analog counterparts with continuously variable positioning enhance functionality in many applications, such as optical switching [3] and spatial light modulators for image projection [4]. Another approach to avoiding the pull-in effect is to use electrode charge instead of electrode voltage to adjust the position. It was shown that when charge is used as the control input instead of voltage, the bifurcation associated with voltage control is eliminated [5].

The complexity of MEMS has increased rapidly and new research areas have emerged such as micromechatronics and microfluidics. The diversity and increase in complexity and integration level of MEMS devices require control techniques and strategies that will make these devices function more efficiently. A few control techniques have been used in the control of MEMS and readily available in the literature; a representative few will be discussed here. A good review of some of the control issues associated with MEMS can be found in [6]. Many researchers designed closed-loop voltage control laws based on the electrode gap; see for example [1]. The authors showed theoretically that the linear position feedback may be used to locally stabilize any point in the gap. The results obtained in [1] were based on local set-point control and moves the electrode through large translations using a series of small step changes. Seeger and Cray [7] showed that every point in the gap may be stabilized by a precisely selected capacitor placed in series with the electrostatic MEMS. Many researchers continued along the same

*Address correspondence to this author at the Mechanical Engineering Department, The Petroleum Institute, Abu Dhabi, UAE; E-mail: mkarkoub@pi.ac.ae

lines of [7] and developed models which account for parasitics and rotational tip-in instability for rigid electrodes [8,9] and for membrane electrodes [7]. Maithripala and his group [10] developed a capacitive stabilization controller for an electrostatic MEMS based on the output feedback control technique. The authors used static charge feedback and showed that it is possible to semi-globally stabilize every point in the gap. While it has been shown that it is not possible to significantly affect mechanical transients using static charge feedback [10], dynamic output feedback may be used instead to stabilize any point of the gap with good transient performance. Wang [11] developed a technique for improvement of the transient performance of a MEMS device consisting of a cantilever beam with double-sided actuation. The author also applied an energy-based control method, and found that velocity feedback is needed. However, it was shown that robust variable-structure approach does not require velocity measurement. Sane *et al.* [11] also applied variable-structure control to an electrostatically-actuated torsional mirror. Although, the authors were able to achieve good results by sensing the mirror angle through large moment arm beam deflections, it was not clear if the presented approach will work outside the laboratory. Zhu *et al.* [12] used a non-linear control technique to improve the performance of a parallel plate electro-static actuator. The control schemes are based on differential flatness, Lyapunov functions, and backstepping. The simulation results showed that the designed controllers were able to stabilize the system as well as attaining a good performance level. Wang *et al.* [11] applied a control law for a MEMS comb resonator to perform impulse disturbance damping and sinusoidal position control. The position feedback signal was produced by a through-wafer optical microbe and used to determine the effective mass, damping, and spring constants. After identifying the model of the MEMS, the authors applied a PID translational controller and proved the controllability of such microstructure. Yunfeng *et al.* [13] used a decoupled control design structure and pole placement technique in the control of a MEMS-based dual stage magnetic disk drive. The authors also analyzed the effect of the microactuator resonance mode variations on the stability and performance of the controller. Dong *et al.* [14] developed an adaptive control system to control both axes of a vibrational MEMS gyroscope. The Lyapunov technique was used to design the controller as well as the adaptive laws and the results were verified through simulations.

Lu and Fedder [15] used capacitance measurements to measure the displacement, and derive a classical linear, time-invariant control law which led to approximately doubling the operational range of a parallel plate capacitor. The transient behavior is addressed through an input-shaping prefilter. Although the proposed technique extends the operational range of the device, stability of the closed-loop is guaranteed locally only. Anderson *et al.* [16] presented a charge and position sensor for electrostatic MEMS. The functionality of the sensor was validated through numerical finite element analysis using ANSYS. The authors also designed a non-linear passivity based controller for the electrostatically actuated MEMS which can be on-chip, local or integrated circuit components. Horenstein *et al.* [17] presented an integrated capacitive position sensor. This sensor is similar the one presented by Anderson *et al.* [16], but it

does not measure charge, and is therefore not suitable for use in the passivity-based feedback controller. Other passive and semi-passive control techniques have also been used in the literature; however, these techniques tend to further complicate the system; see for example [7] and [18]. In this paper controllers based on the sliding mode technique will be designed for an electro-static actuator. This technique has been successfully used with nonlinear dynamic systems and good results were achieved; see for example [19]

The rest of the paper is organized as follows: The dynamic model of an electrostatic MEMS with one mechanical translational degree of freedom is presented in section 2. The model consists of three-parallel plate capacitor with the middle plate movable and the top and bottom plates fixed. A linear spring and a viscous damper are used in the system to represent the flexible support holding the top. A few assumptions have been made in order to obtain the equations of motion of the electrostatic MEMS such as no stiction and no electrical shorting. The latter effect could be guaranteed by having an insulating layer of pre-specified thickness on the bottom plate. It is assumed that the voltage across the electrodes and the charge or the capacitance of the device are measurable. Three control techniques are presented in Sections 3, 4, and 5. We begin by designing a feedback linearization controller for the electrostatic MEMS in section 3. A second controller based on the sliding mode technique is designed in section 4. Finally, a dynamic sliding mode control law is derived in section 5. The simulation results of all three controllers are presented in section 6. Finally, some concluding remarks are given in section 7.

DYNAMIC MODEL OF THE ELECTROSTATIC MICRO-ELECTROMECHANICAL SYSTEM

Many microelectromechanical systems (MEMS) rely on parallel-plate electrostatic microactuators. These actuators have two fixed plates at the top and bottom of the device and one movable plate in the middle. The actuation principle behind this type of actuators is the attractive force of two oppositely charged plates resulting from applying a voltage between them. For transverse drive electrostatic microactuators, the electrostatic force is a nonlinear function of the gap and the applied voltage. It is worth mentioning that the electrostatic force has an inherent negative spring constant. To ensure small motion stability of the device, the movable plate is suspended *via* mechanical elastic members, spring and damper, see Fig. (1) In this section, the theoretical model for a parallel-plate electrostatic microactuator is derived.

Consider the one-dimensional schematic diagram of an electrostatic microactuator shown in Fig. (1).

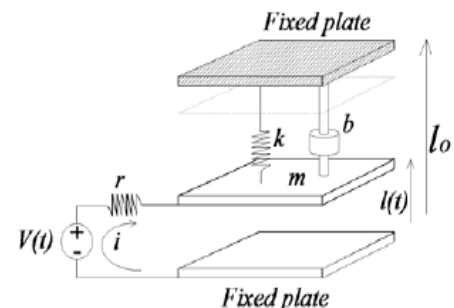


Fig. (1). Schematic diagram of an electrostatic microactuator.

The following variables are used throughout the paper.

A : Cross-sectional area of each of the electrodes;

b : Damping coefficient;

$i(t)$: Current through the device;

k : Linear spring constant;

$l(t)$: Gap between the electrodes;

l_0 : Zero voltage gap;

ζ : Damping ratio;

σ : Positive real number;

\bar{l}_o : Normalized zero voltage gap;

m : Mass of the movable electrode;

Q : Charge on a electrode;

r : Electrical resistance in the circuit;

t : Time;

\hat{t} : Normalized time;

u : Normalized control voltage;

v : Control voltage;

x : Normalized state vector;

x_1 : Normalized charge;

x_{1d} : Normalized desired equilibrium charge;

x_2 : Normalized gap;

x_{2d} : Normalized desired equilibrium gap;

x_3 : Normalized velocity.

The capacitance of the device is equal to $\varepsilon A/l(t)$. The attractive electrostatic force on the top plate is $Q^2(t)/2\varepsilon A$. The current through the input resistance r is

$$i(t) = \frac{1}{r} \left(v(t) - \frac{Q(t)l(t)}{\varepsilon A} \right)$$

The equations of motion in the form given by Senturia [20]

$$m\ddot{l}(t) = bl(t) - k(l(t) - l_0) - \frac{Q(t)l(t)}{\varepsilon A} \quad (1)$$

$$\dot{Q}(t) = \frac{1}{r} \left(v(t) - \frac{Q(t)l(t)}{\varepsilon A} \right) \quad (2)$$

Normalizing the time scale such that $\hat{t} = \sigma t$ and define

$v = r\sigma\beta u$, $\alpha = \varepsilon A r \sigma$, $\beta = \varepsilon A \sigma \sqrt{m r \sigma}$ and let the normalized state vector x be such that:

$$x = \begin{bmatrix} x_1 \\ x_2 \\ x_3 \end{bmatrix} = \begin{bmatrix} Q/\beta \\ l/\alpha \\ i/\alpha \end{bmatrix} \quad (3)$$

The dynamic model of the electrostatic microelectromechanical system can be described by the following set of ordinary differential equations [20]:

$$\begin{aligned} \dot{x}_1 &= -x_1 x_2 + u \\ \dot{x}_2 &= x_3 \\ \dot{x}_3 &= -2\zeta\omega x_3 - \omega^2(x_2 - \bar{l}_o) - \frac{1}{2}x_1^2 \end{aligned} \quad (4)$$

The objective of the control scheme is to regulate x to its desired value x_d . The constant desired value of x is such that,

$$x_d = \begin{bmatrix} x_{1d} \\ x_{2d} \\ x_{3d} \end{bmatrix} = \begin{bmatrix} x_{1d} \\ -\frac{1}{2\omega^2}x_{1d}^2 + \bar{l}_o \\ 0 \end{bmatrix} \quad (5)$$

Consider the change of variables $z = T(x)$, with $z = [z_1 \ z_2 \ z_3]^T$ such that,

$$\begin{aligned} z_1 &= x_2 - x_{2d} \\ z_2 &= x_3 \\ z_3 &= -2\zeta\omega x_3 - \omega^2(x_2 - \bar{l}_o) - \frac{1}{2}x_1^2 \end{aligned} \quad (6)$$

Remark 1

Using (5)-(6), it is easy to check that if $z(t)$ converges to zero as $t \rightarrow \infty$, then the states $x_1(t)$ and $x_2(t)$ converge to their desired values $x_{1d}(t)$ and $x_{2d}(t)$ as $t \rightarrow \infty$ and $x_3(t)$ converges to 0 as $t \rightarrow \infty$.

Using (4) and (6), the equations of the motor can be written as functions of the new variables z_1 , z_2 and z_3 such that,

$$\begin{aligned} \dot{z}_1 &= z_2 \\ \dot{z}_2 &= z_3 \\ \dot{z}_3 &= f + gu \end{aligned} \quad (7)$$

where

$$\begin{aligned} f &= -2\zeta\omega \left[-2\zeta\omega x_3 - \omega^2(x_2 - \bar{l}_o) - \frac{1}{2}x_1^2 \right] \\ &\quad - \omega^2 x_3 + x_1^2 x_2 \\ &= (4\zeta^2 - 1)\omega^2 x_3 + 2\zeta\omega^3(x_2 - \bar{l}_o) \\ &\quad + \zeta\omega x_1^2 + x_1^2 x_2 \end{aligned} \quad (8)$$

$$g = -x_1 \quad (9)$$

In the upcoming sections, three controllers will be designed for the electrostatic microelectromechanical actuator using the control diagram shown in Fig. (2).

DESIGN OF A FEEDBACK LINEARIZATION CONTROLLER

Let α_1 , α_2 and α_3 be positive scalars such that the polynomial $P_I(s) = s^3 + \alpha_3 s^2 + \alpha_2 s + \alpha_1$ is Hurwitz.

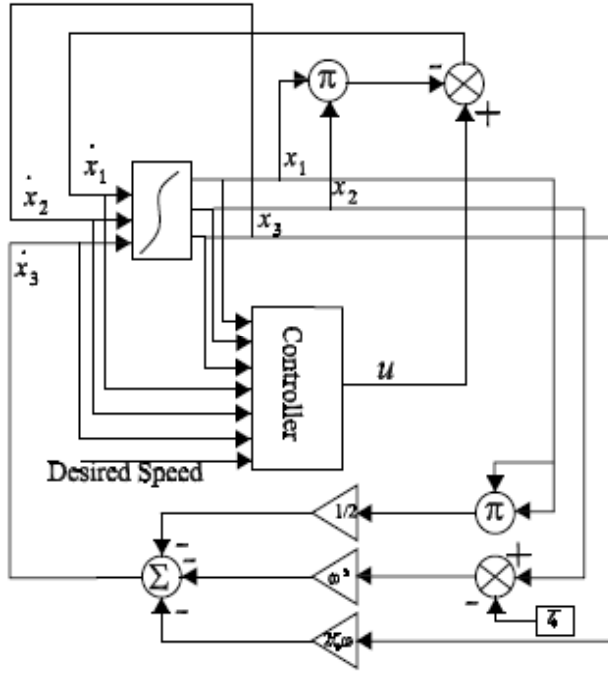


Fig. (2). Control diagram for the electrostatic microactuator.

Proposition 1

The controller

$$u = \frac{1}{g}(-f - \alpha_1 z_1 - \alpha_2 z_2 - \alpha_3 z_3) \quad (10)$$

when applied to the transformed microelectromechanical system (7) guarantees the asymptotic convergence of the states

$z(t)$ to zero as $t \rightarrow \infty$.

Proof

The closed loop system when the controller (10) is applied to the microelectromechanical system (7) is such:

$$\dot{z} = A_{cl} z \quad (11)$$

with

$$A_{cl} = \begin{bmatrix} 0 & 1 & 0 \\ 0 & 0 & 1 \\ -\alpha_1 & -\alpha_2 & -\alpha_3 \end{bmatrix} \quad (12)$$

The solution of the above equation is $z(t) = \exp(A_{cl}t)z(0)$. Since A_{cl} is a stable matrix, then $z(t)$ converges to zero as $t \rightarrow \infty$. It should be mentioned that since $z(t)$ converges to zero as $t \rightarrow \infty$, then the states of the system will converge to their desired values as $t \rightarrow \infty$.

Remark 2

The controller (10) can be written as a function of the coordinates x_1 , x_2 and x_3 such that

$$u = \frac{1}{g} \left(-f - \alpha_1 (x_2 - x_{2d}) - \alpha_2 x_3 + \alpha_3 \left(2\zeta\omega x_3 + \omega^2 (x_2 - \bar{l}_o) + \frac{1}{2} x_1^2 \right) \right) \quad (13)$$

DESIGN OF SLIDING MODE CONTROLLERS FOR THE SYSTEM

Design of a Static Sliding Mode Controller

The design of a sliding mode control scheme for the system is discussed in this section.

The first step in designing a sliding mode control scheme for the system is to design the switching surface. Let the switching surface S be such that,

$$\begin{aligned} S &= z_3 + \lambda_1 z_2 + \lambda_2 z_1 \\ &= -2\zeta\omega x_3 - \omega^2 (x_2 - \bar{l}_o) - \frac{1}{2} x_1^2 + \lambda_1 x_3 \\ &\quad + \lambda_2 (x_2 - x_{2d}) \end{aligned} \quad (14)$$

where λ_1 and λ_2 are positive scalars. Let W be a positive scalar.

Proposition 2

The following sliding mode controller:

$$u = \frac{1}{g} \left(-f - \lambda_1 z_3 - \lambda_2 z_2 + W \text{sign}(z_3 + \lambda_1 z_2 + \lambda_2 z_1) \right) \quad (15)$$

when applied to the microelectromechanical system, guarantees the convergence of z_1 , z_2 and z_3 to 0

as $t \rightarrow \infty$.

Proof

Differentiating (14) with respect to time and using (7), it follows that,

$$\begin{aligned} \dot{S} &= \dot{z}_3 + \lambda_1 \dot{z}_2 + \lambda_2 \dot{z}_1 \\ &= f + gu + \lambda_1 z_3 + \lambda_2 z_2 \end{aligned} \quad (16)$$

Substituting u by its value from (15) and using (14), it follows that,

$$\begin{aligned} \dot{S} &= f + gu + \lambda_1 z_3 + \lambda_2 z_2 \\ &= -W \text{sign}(z_3 + \lambda_1 z_2 + \lambda_2 z_1) \\ &= -W \text{sign}(S) \end{aligned} \quad (17)$$

It is a well known fact that, to guarantee switching, we need to have $S\dot{S} < 0$. It can be easily checked that the dynamics in (17) guarantees that $S\dot{S} < 0$. The trajectories associated with the unforced discontinuous dynamics (17) exhibit a finite time reachability to zero from any given initial condition $S(0)$ provided that the constant gain W is chosen to be large enough strictly positive. Since S is driven to zero in

finite time, the reduced order model of the system is governed after such finite amount of time by,

$$\dot{z}_r = A_{c2} z_r \quad (18)$$

where

$$A_{c2} = \begin{bmatrix} 0 & 1 \\ -\lambda_2 & -\lambda_1 \end{bmatrix} \quad z_r = \begin{bmatrix} z_1 \\ z_2 \end{bmatrix}$$

The matrix A_{c2} is a stable matrix because the scalars λ_1 and λ_2 are chosen to be positive scalars. Since A_{c2} is a stable matrix, then equation (18) implies that $z_r(t)$ will asymptotically converge to zero. Since z_1 and z_2 asymptotically converge to zero, then because of the choice of the sliding surface given in (14), z_3 will also asymptotically converge to zero. Therefore, the controller (15) guarantee the asymptotic convergence of the states $x_1(t)$ and $x_2(t)$ to their desired values $x_{1d}(t)$ and $x_{2d}(t)$ as $t \rightarrow \infty$ and the convergence of $x_3(t)$ to 0 as $t \rightarrow \infty$.

To avoid the chattering associated with sliding mode controllers, we will use the hyperbolic tangent instead of the sign function in the controller given by Proposition 2.

Proposition 3

The following sliding mode controller:

$$u = \frac{1}{g} \left(-f - \lambda_1 z_3 - \lambda_2 z_2 - W \tanh(z_3 + \lambda_1 z_2 + \lambda_2 z_1) \right) \quad (19)$$

when applied to the microelectromechanical system, guarantees the convergence of z_1 , z_2 and z_3 to 0 as t goes to infinity.

Proof

Let the Lyapunov function be such that V be such that

$$V = \frac{1}{2} S^2 \quad (20)$$

Taking the derivative of V with respect of time, it follows that:

$$\dot{V} = S\dot{S} = -WS \tanh(s) \quad (21)$$

Since W is chosen to be positive, it follows that $\dot{V} < 0$ for $S \neq 0$ and $\dot{V} = 0$ for $S = 0$. Therefore, it can be concluded that the dynamics

$$\dot{S} = -W \tanh(S) \quad (22)$$

guarantees the reachability to the surface $S = 0$. The rest of the proof is the same as the one for Proposition 2.

Remark 3

The controller (19) can be written as a function of the coordinates x_1 , x_2 and x_3 such that

$$u = \frac{1}{g} \left(-f + \lambda_1 \left(2\zeta\omega x_3 + \omega^2 (x_2 - \bar{l}_o) + \frac{1}{2} x_1^2 \right) - \lambda_2 x_3 - W \tanh(S) \right) \quad (23)$$

with

$$S = -2\zeta\omega x_3 - \omega^2 (x_2 - \bar{l}_o) - \frac{1}{2} x_1^2 + \lambda_1 x_3 + \lambda_2 (x_2 - x_{2d}) \quad (24)$$

DESIGN OF A DYNAMIC SLIDING MODE CONTROLLER

To reduce the chattering due to the static sliding mode controller, a dynamic sliding mode controller is proposed in this section.

Let the output of the system be such that:

$$y = z_1 \quad (25)$$

Differentiating (25) with respect to time four times, it follows that,

$$y^{(4)} = \dot{f} + \dot{g}u + g\ddot{u} \quad (26)$$

where

$$\dot{f} = (1 - 4\zeta^2)\omega^2 \left(2\zeta\omega x_3 + \omega^2 (x_2 - \bar{l}_o) + \frac{1}{2} x_1^2 \right) + 2\zeta\omega^3 x_3 + 2(\zeta\omega + x_2)(-x_1 x_2 + u)x_1 + x_1^2 x_3 \quad (27)$$

$$\dot{g} = x_1 x_2 - u \quad (28)$$

We will choose the switching surface Γ such that,

$$\Gamma = y^{(3)} + \gamma_1 \ddot{y} + \gamma_2 \dot{y} + \gamma_3 y \quad (29)$$

where γ_1 , γ_2 and γ_3 are positive design parameters which are chosen such that the polynomial $P_2(s) = s^3 + \gamma_1 s^2 + \gamma_2 s + \gamma_3$ is a Hurwitz polynomial. Using (29), (25) and (6), the switching surface σ can be written as,

$$\Gamma = f + gu - \gamma_1 \left(2\zeta\omega x_3 + \omega^2 (x_2 - \bar{l}_o) + \frac{1}{2} x_1^2 \right) + \gamma_2 x_3 + \gamma_3 (x_2 - x_{2d}) \quad (30)$$

Let W_d be a positive scalar.

Proposition 4

The following discontinuous dynamic control scheme,

$$\dot{u} = \frac{1}{g} \left(-\dot{f} - g\ddot{u} - \gamma_1 (f + gu) - \gamma_3 x_3 - W_d \text{sign}(\Gamma) + \gamma_2 \left(2\zeta\omega x_3 + \omega^2 (x_2 - \bar{l}_o) + \frac{1}{2} x_1^2 \right) \right) \quad (31)$$

when applied to the microelectromechanical system, asymptotically stabilizes the states to their desired values.

Proof

Differentiating (29) with respect to time and using (26), (25) and (6), it follows that,

$$\begin{aligned} \dot{\Gamma} &= y^{(4)} + \gamma_1 y^{(3)} + \gamma_2 \ddot{y} + \gamma_3 \dot{y} \\ &= \dot{f} + g\ddot{u} + \dot{g}u + \gamma_1 (f + gu) + \gamma_3 x_3 \\ &\quad - \gamma_2 \left(2\zeta\omega x_3 + \omega^2 (x_2 - \bar{l}_o) + \frac{1}{2} x_1^2 \right) \end{aligned} \quad (32)$$

Substituting \dot{u} by its value from (31), we get,

$$\begin{aligned} \dot{\Gamma} &= \dot{f} + \dot{g}u + \gamma_1(f + gu) + \gamma_3x_3 \\ &\quad - \gamma_2 \left(2\zeta\omega x_3 + \omega^2(x_2 - \bar{l}_o) + \frac{1}{2}x_1^2 \right) \\ &\quad + (-\dot{f} - \dot{g}u - \gamma_1(f + gu) - \gamma_3x_3 - W_d \text{sign}(\Gamma) \\ &\quad + \gamma_2 \left(2\zeta\omega x_3 + \omega^2(x_2 - \bar{l}_o) + \frac{1}{2}x_1^2 \right)) \\ &= -W_d \text{sign}(\Gamma) \end{aligned} \tag{33}$$

To guarantee switching, we need to have $\Gamma\dot{\Gamma} < 0$. It can be easily checked that the dynamics in (33) guarantees that $\Gamma\dot{\Gamma} < 0$. The trajectories associated with the unforced discontinuous dynamics (33) exhibit a finite time reachability to zero from any given initial condition $\Gamma(0)$ provided that the constant gain W_d is chosen to be strictly positive. Since Γ is driven to zero in finite time, the output $y = z_1$ is governed after such finite amount of time by the third order differential equation $\ddot{y} + \gamma_1\dot{y} + \gamma_2y + \gamma_3y = 0$. Thus the output $y(t) = z_1$ will converge to zero because γ_1, γ_2 and γ_3 are positive scalars such that $P_2(s) = s^3 + \gamma_1s^2 + \gamma_2s + \gamma_3$ is a Hurwitz polynomial. Since z_1 converges to zero, then z_2 and z_3 will also converge to zero. Thus x_1, x_2 , and x_3 will also converge to their desired values.

Therefore, it can be concluded that the dynamic sliding mode controller given by (31) guarantees the asymptotic convergence of the states to their desired values.

SIMULATION RESULTS

The closed-loop system described by (2) or (7) and one of the controllers (10), (15), (19), or (31) is analyzed through computer simulations. The normalized natural frequency of the system is $\omega = 1$ and the damping ratio $\zeta = 0$; a worst case scenario in terms of damping. The normalized zero voltage gap is taken as $\bar{l}_0 = 1$ and a nominal gap $x_{2d} = 0.2$ is stabilized by each of the proposed control schemes.

Simulation Results for the Feedback Linearization Controller

Two sets of values for α_1, α_2 , and α_3 are used. In the first set, we used $\alpha_1 = 0.0013, \alpha_2 = 0.0362$, and $\alpha_3 = 0.33$ (corresponding to three real closed loop poles located at $-0.1, -0.11$ and -0.12). In the second set, we used $\alpha_1 = 0.2, \alpha_2 = 2.02$, and $\alpha_3 = 0.3$ (corresponding to one real and two complex closed loop poles located at $-0.1, -0.1 + j1.41$ and $-0.1 - j1.41$).

The simulation results for the feedback linearization controller are given in Figs. (3)-(6). In the figures, the dashed lines correspond to the first set of α 's and the continuous lines correspond to the second set of α 's.

The figures indicate that the proposed feedback controller works well for the regulation of the microelectromechanical system. It is clear that the system is more sluggish with first set of α 's and that is expected due to the location of the closed-loop poles. Although the time response is a little slow overall, the normalized maximum control voltage is rela-

tively low (< 1). This is an attractive feature of the proposed control scheme.

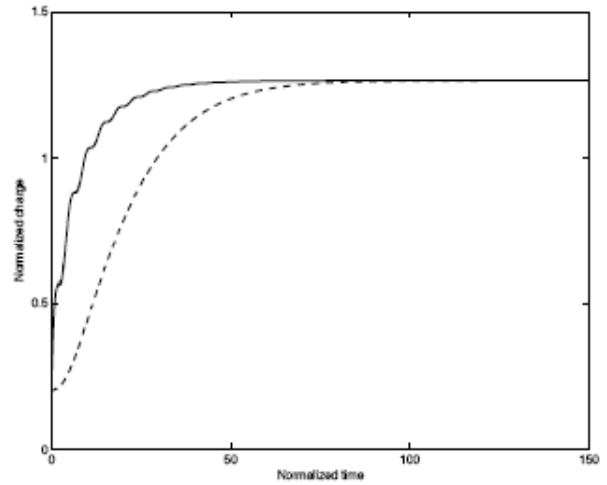


Fig. (3). The Normalized charge versus normalized time when the F.L. controller is used: (solid): first set of α 's and (dashed): second set of α 's.

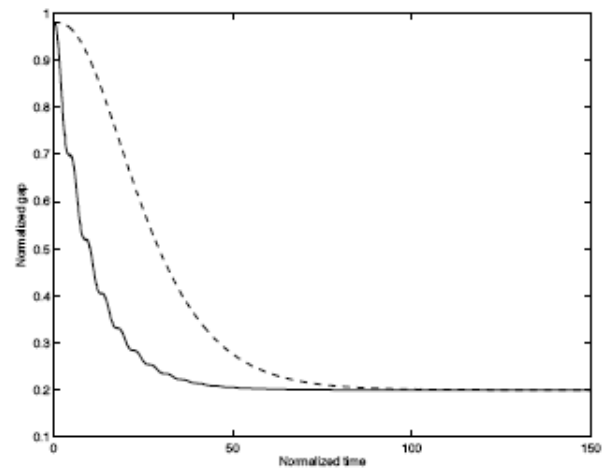


Fig. (4). The Normalized gap versus normalized time when the F.L. controller is used: (solid): first set of α 's and (dashed): second set of α 's.

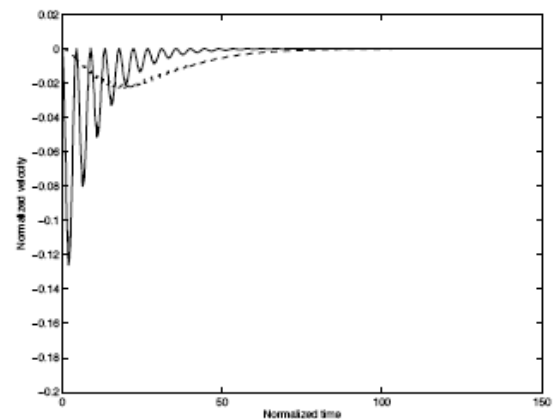


Fig. (5). The Normalized velocity versus normalized time when the F.L. controller is used: (solid): first set of α 's and (dashed): second set of α 's.

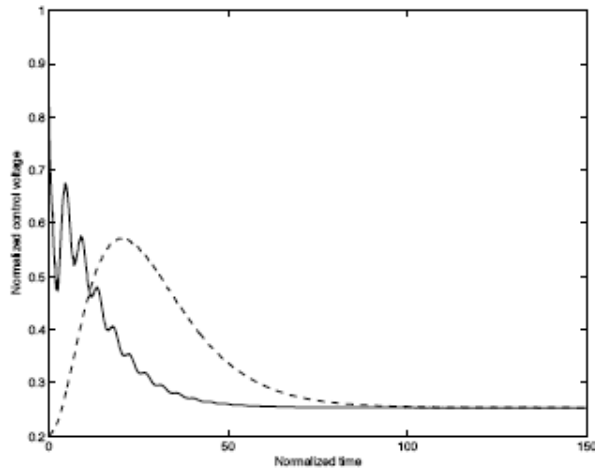


Fig. (6). The Normalized control voltage versus normalized time when the F.L. controller is used: (solid): first set of α 's and (dashed): second set of α 's.

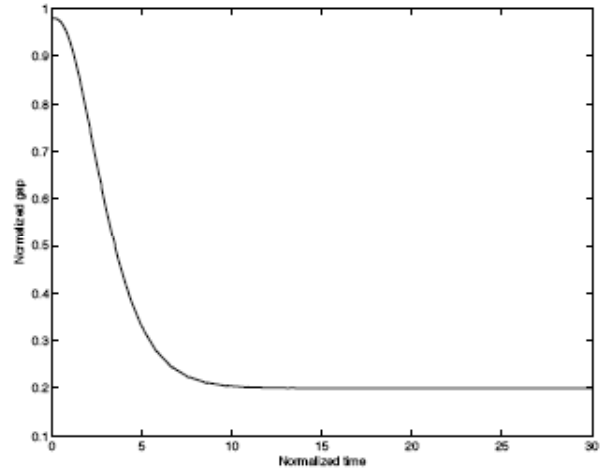


Fig. (8). The Normalized gap versus normalized time when the S.S.M controller is used.

Simulation Results for the Static Sliding Mode Controller

The static sliding mode controller is used to control the electrostatic actuator and the simulation results are presented here. The parameters of the static sliding mode controller are $\lambda_1=1.8$, $\lambda_2=0.8$, and $W=1$. The simulation results for the static sliding mode controller (23)- (24) are given in Figs. (7)-(10). The figures indicate that the proposed static sliding mode controller works well for the regulation of the microelectromechanical system. The normalized time response is faster than that of the closed-loop system described in Section 3. However, the maximum normalized voltage has almost doubled (<2).

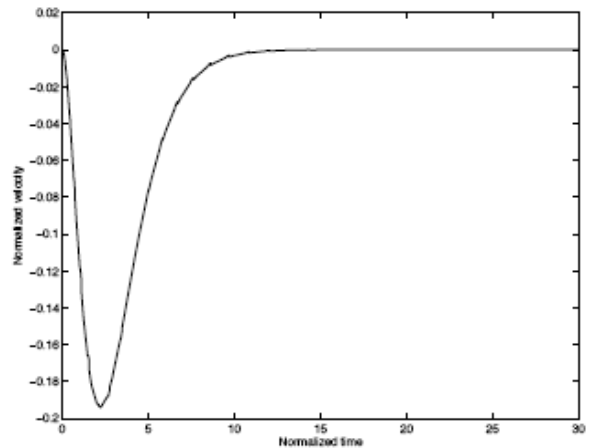


Fig. (9). The Normalized velocity versus normalized time when the S.S.M controller is used.

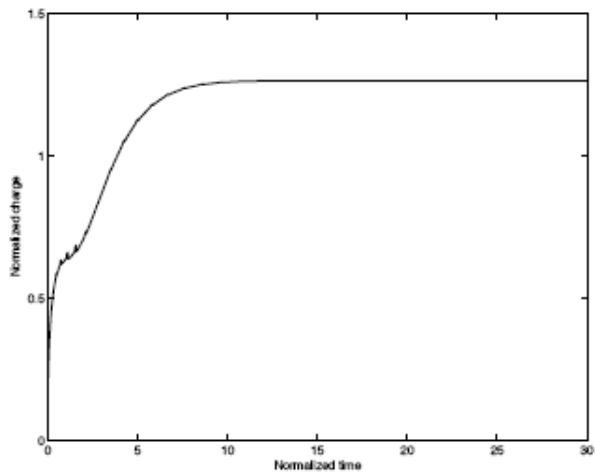


Fig. (7). The Normalized charge versus normalized time when the S.S.M controller is used.

Simulation Results for the Dynamic Sliding Mode Controller

Finally, the electrostatic actuator closed-loop system is simulated using the dynamic sliding mode controller (31) and the results are given in Figs. (11)-(14). The parameters of the dynamic sliding mode controller are $\gamma_1=7.8$, $\gamma_2=20.27$,

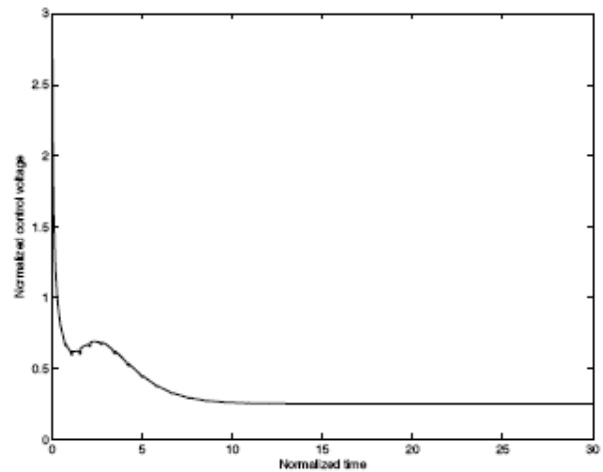


Fig. (10). The Normalized control voltage versus normalized time when the S.S.M controller is used.

$\gamma_3=17.55$ and $W_d=8$. The simulation results for the dynamic sliding mode controller (31) are given in Figs. (11)-(14).

The figures indicate that the proposed static sliding mode controller works well for the regulation of the microelectromechanical system. The normalized time response as well as the normalized voltage appear to be similar to those presented in Section 4.1.

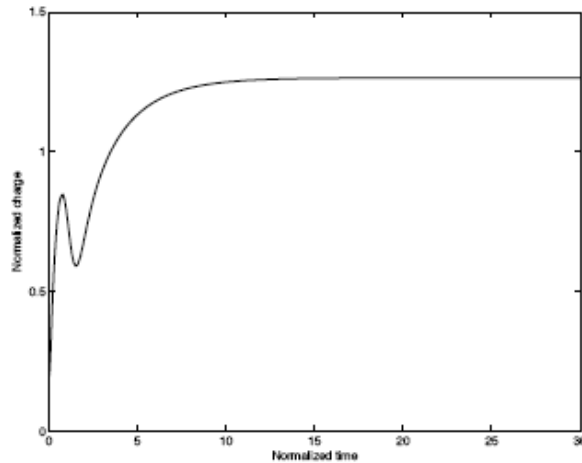


Fig. (11). The Normalized charge versus normalized time when the D.S.M controller is used.

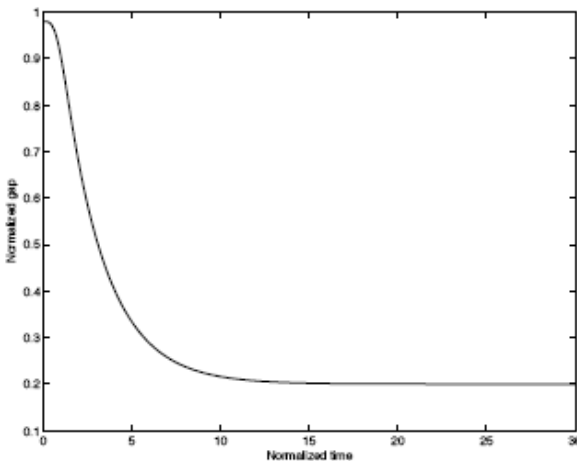


Fig. (12). The Normalized gap versus normalized time when the D.S.M controller is used.

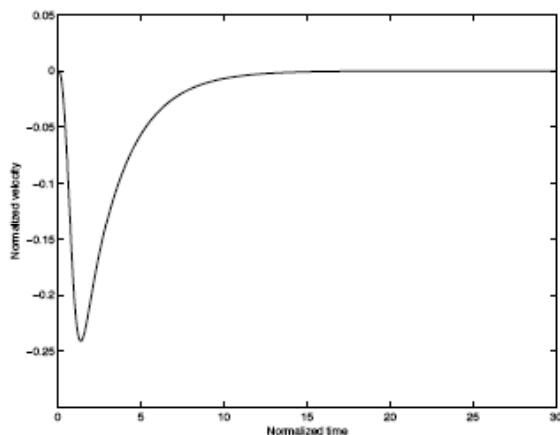


Fig. (13). The Normalized velocity versus normalized time when the D.S.M controller is used.

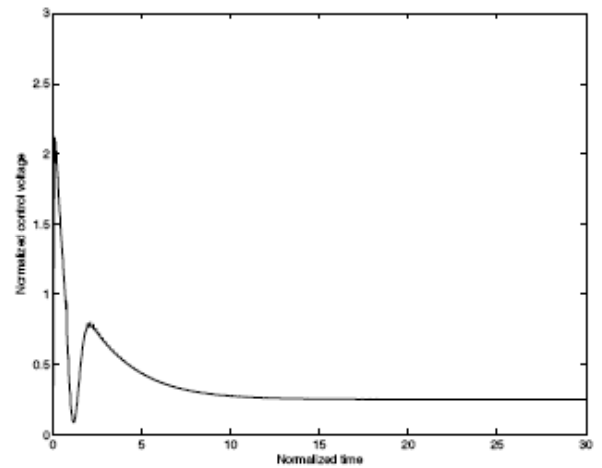


Fig. (14). The Normalized control voltage versus normalized time when the D.S.M controller is used.

CONCLUSION

Three nonlinear controllers are proposed for a microelectromechanical system. The controllers are a feedback linearization controller, a static and a dynamic feedback controllers. It is proved that the proposed controllers guarantee the asymptotic regulations of the states of the microelectromechanical system to their desired values. Simulation results are presented to show the effectiveness of the proposed control schemes.

Future research will address the implementation of the proposed control schemes on an experimental setup.

REFERENCES

- [1] Chu PB, Pister SJ. 1994, Analysis of Closed-loop Control of Parallel-Plate Electrostatic MicroGrippers, Proceeding of the IEEE International Conference on Robotics and Automation, 1994: 820-825.
- [2] Hornbeck LJ. From cathode rays to digital micromirrors: A history of electronic projection display technology, TI Technical Journal, July-September, 1998: 7-46.
- [3] Comtois J, Michalick A, Cowan W, Butler J. Surface-micromachined Polysilicon MOEMS for Adaptive Optics, Sensors and Actuators A, 1999: 78, 54-62.
- [4] Kovacs GTA. Micromachined Transducers Sourcebook, McGraw-Hill, New York; 1998.
- [5] Nadal-Guardia R, Dehe A, Aigner RLM. Castaner, 2002, Current drive methods to extend the range of travel of electrostatic microactuators beyond the voltage pull-in point, J Microelectromech Sys 2002; 11(3): 255-263.
- [6] Bryzek J, Abbott E, 2003, Control Issues for MEMS, Proceedings of the 42nd IEEE Conference on Decision and Control, Maui, Hawaii, 1997: 3039-3057.
- [7] Seeger JL, Crary SB. Stabilization of Electrostatically Actuated Mechanical Devices, Proc. of the Ninth Int. Conf. on Solid-State Sensors and Actuators (Transducers '97), Chicago, IL, June 16-19, 1997: 1133-1136.
- [8] Chan EK, Dutton RW. Electrostatic micromechanical actuator with extended range of travel, J Microelectromechanical Sys 2000; 9(3): 321-328.
- [9] Pelesko JA, Triolo AA, Nonlocal Problems in MEMS Device Control, J Eng Mathe 2001; 41(4): 345-366.
- [10] Maithripala DHS, Berg JM, Dayawansa WP, Control of an Electrostatic MEMS Using Static and Dynamic Output Feedback, ASME J Dyna Sys Measu Control 2005; 127: 443-450.
- [11] Wang PKC. Feedback Control of Vibrations in a Micromachined Cantilever Beam with Electrostatic Actuators, J Sou Vibration 1998; vol. 213(3): 537-550.

- [12] Zhu G, Levine J, Praly. Improving the Performancd of an Electrostatically Actuated MEMS by Nonlinear Control: Some Advances and Comparisons, Proceedings of the IEEE Conference on Decision and Control and the European Control Conference, Seville, Spain, 2005: 7534-7539.
- [13] Yunfeng L, Horowitz R. Mechatronics of Electrostatic Microactuators for Computer Disk Drive Dual-Stage Servo Sytems, IEEE/ASME Transactions on Mechatronics, 2001; 6(2): 111-121.
- [14] Dong L, Leland R. The Adaptive Control System of a MEMS Gyroscope with Time Varying Rotation Rate, Proceedings of the American Control Conference, Portland, Oregon; 2005: 3592-3597.
- [15] Lu, M S-C, Fedder G K. Position Control of Parallel-Plate Microactuators for Probe-Based Data Storage, J Microelectromechanical Sys 2004; 13(5): 759-769.
- [16] Anderson RC, Kawade B, Maithripala DHS, Ragulan K, Berg JM, Gale RO. Integrated charge sensors for feedback control of electrostatic MEMS, Proceedings of the SPIE conference on Smart Structures and Materials: Sensors and Smart Structures Technologies for Civil, Mechanical, and Aerospace Systems, San Diego, 2005.
- [17] Horenstein MN, Perreault JA, Bifano TG. Differential capacitive position sensor for planar MEMS structures with vertical motion, Sensors Actuators 2000; 80: 53-61.
- [18] Kynarainen JM, Oja AS, Seppa, H. Increasing the Dynamic Range of a Micromechanical Moving-Plate Capacitor, J of Analog Integra Cir Sig Processing, 2001; 29: 61-70.
- [19] Karkoub MA, Zribi M. Robust Control Schemes for an Overhead Crane, J Vibra Cont, 2001; 7: 395-416.
- [20] Senturia SD. Microsystem Design, Kluwer Academic Publishers: Norwell, MA: 2001.

Received: January 23, 2008

Revised: March 13, 2008

Accepted: March 19, 2008

© Karkoub and Zribi; Licensee *Bentham Open*.

This is an open access article licensed under the terms of the Creative Commons Attribution Non-Commercial License (<http://creativecommons.org/licenses/by-nc/3.0/>) which permits unrestricted, non-commercial use, distribution and reproduction in any medium, provided the work is properly cited.